The role of retained austenite in the hydrogen embrittlement of quenching and partitioning (Q&P) steels

Simon Vander Vennet[1], **Silvia Leitner**[2], **Vsevolod Razumovskiy**[2], **Werner Ecker**[2], **Tom Depover**[1], **Kim Verbeken**[1]

[1]*Ghent University, Department of Materials, Textiles and Chemical Engineering, Research group Sustainable Materials Science, Ghent, Belgium*
simon.vandervennet@ugent.be, tom.depover@ugent.be, kim.verbeken@ugent.be

[2]*Materials Center Leoben Forschung GmbH (MCL), Leoben, Austria*
silvia.leitner@mcl.at, vsevolod.razumovskiy@mcl.at, werner.ecker@mcl.at

Abstract

This work investigates the effect of a constant load on hydrogen diffusion through a Q&P steel containing metastable retained austenite by combining electrochemical hydrogen permeation and thermal desorption spectroscopy. Material samples are placed under different external loading conditions, ranging from 50% to 125% of the yield stress. The permeation transients indicate that hydrogen diffusion in this Q&P-steel is delayed under all stressed conditions, even at stresses in the elastic regime, with the delay increasing with the applied load. From thermal desorption spectroscopy performed on the same specimens after the permeation test appears that the samples tested under load show a high temperature peak which is not present in the unloaded sample. Thus indicating that the retained austenite is capable of trapping hydrogen in a loaded condition.

Keywords: Hydrogen permeation; Hydrogen diffusion; Mechanical load; Retained austenite; Quenching and partitioning

Introduction

Quenching & Partitioning (Q&P) steels are part of the third generation advanced high strength steels (AHSS) and were proposed by Edmonds et al. [1] as an alternative for transformation induced plasticity (TRIP)-assisted and dual phase (DP) steel in automotive applications. The final microstructure of Q&P steel consists of intercritical ferrite (α) and/or martensite (α') combined with retained austenite with a significantly increased carbon content compared to the matrix [2]. The increased carbon content is achieved by allowing carbon diffusion into the austenite (γ) during the heat treatment (partitioning) and is necessary to stabilise the austenite during the final quenching step down to room temperature. The retained austenite is metastable at room temperature and provides increased ductility by the TRIP-effect.

However, one of the main drawbacks of high strength steels is their susceptibility to hydrogen embrittlement [3–5] and Q&P steel is no exception to this [6–8]. Retained austenite plays a crucial role in this story, since it has both advantages and disadvantages with respect to hydrogen. At first sight, it would seem that retained austenite is advantageous against hydrogen embrittlement due to its high solubility and low diffusivity [9, 10], thereby effectively serving as a strong trapping site. Under the assumption that retained austenite remains stable in the material, it should indeed be considered as a beneficial trapping site. However, when it transforms into martensite due to an applied stress, the assumption of a stable austenite phase is no longer valid. In this case, the high solubility becomes a disadvantage as upon transformation, the hydrogen that was dissolved in the austenite phase is inherited by the brittle fresh martensite, which has a considerably lower hydrogen solubility [11, 12].

Additionally, the fresh martensite shows an increased susceptibility to hydrogen embrittlement due to its high dislocation density and residual stresses [13]. Previous studies on the hydrogen embrittlement of Q&P steel already showed that the interface between retained austenite and ferrite/martensite is a preferential initiation site for transgranular cracks [6, 7]. Therefore, understanding the interplay between hydrogen diffusion into retained austenite, the stability of retained austenite, and stress is crucial in assessing the hydrogen embrittlement of Q&P steel. The lack of understanding is illustrated by the fact that some authors observed embrittlement related to retained austenite in Q&P and TRIP-assisted steels without observing hydrogen trapping, whereas other authors did report trapping by retained austenite during electrochemical charging [7, 14]. Considering the ambiguity in these studies [6, 7, 12, 14–16], there seems to be no generally accepted concept of hydrogen trapping by retained austenite.

Furthermore, the interplay between stress and hydrogen diffusion was illustrated by multiple studies using electrochemical hydrogen permeation [17–19]. Van den Eeckhout et al. [17] demonstrated the effect of stress by conducting permeation experiments on dual phase (DP) steel stressed under constant load at different fractions of the yield stress. They found that diffusivity increased with increasing elastic stress, similar to the results by Zhao et al. [18]. Their proposed explanation for this observation is the increase of the volume of the unit cell due to the applied elastic stress, which also causes an expansion of the interstitial sites, thus facilitating hydrogen diffusion. When the constant load applied on the specimen exceeded 100% of the yield stress, diffusivity decreased again due to the formation of lattice defects, such as dislocations, which act as hydrogen traps and slow down diffusion.

In this study, a methodological approach will be used to characterise the interplay between stress and hydrogen diffusion, combined with its effect on trapping in retained austenite and the stability of retained austenite under stress. Samples of Q&P steels will be subjected to permeation experiments under constant load, combined with the assessment of trapping using TDS. Further characterisation of the retained austenite will be performed using scanning electron microscopy, electron backscatter diffraction (SEM-EBSD), and X-ray diffraction (XRD).

Materials and methods

Material characterisation

For this study, a commercial Q&P 980 steel with chemical composition Fe-0.22C-2.33Mn-1.60Si-0.05Al (in wt%) was used. The microstructure of the material was characterised using scanning electron microscopy electron backscatter diffraction (SEM-EBSD, FEI Quanta 450 FEG) operated at an accelerating voltage of 20 kV and a spot size of 5 nm. The EBSD examinations were performed on the normal direction (ND) plane tilted 70° at a working distance of 15 mm and with a step size of 50 nm on a hexagonal grid. After conventional mechanical grinding the samples were polished using 3 μm and 1 μm diamond paste suspension for 5 and 10 minutes, respectively, followed by 30 minutes of polishing with 0.04 μm colloidal silica (Struers OPU suspension) and cleaning with water and ethanol. TSL OIM Data Analysis V7 software was used for post processing and analysis of the obtained data.

As a second method to determine the retained austenite fraction, X-ray diffraction (XRD) was used. These experiments were performed on a Siemens Kristalloflex D5000 diffractometer with a Mo-K$_\alpha$ source operated at 40 kV and 40 mA. The spectra are measured over a range of 2θ from 25° to 40° with a step size of 0.01° and dwell time of 5 s.

Hydrogen/material interaction

Hydrogen permeation was carried out using a set-up based on the Devanathan-Stachurski cell [20] modified with an external loading device. Samples for this method were rectangular with a thickness of 0.85 mm, a width of 25 mm and a length of 90 mm. The clamped edges were sandblasted to improve surface friction between the clamps and the sample. To apply the load during the permeation test, the sample was first mounted in a proof ring manufactured by CORMET®. After clamping, the tensile load was applied by compressing the ring and the actual force could then be determined from the load amplifier.

Deaerated 0.1 M NaOH was used as the electrolyte in both the charging and oxidation cell. After mounting, the anodic side of the sample was placed at a potential of -500 mV relative to a Hg/Hg_2SO_4 reference electrode. This allowed the formation of a passive iron-oxide layer [21]. In case of a permeation test on a specimen placed at a certain load, the oxide layer is formed after applying the load, therefore avoiding damage of the layer during loading. Charging was started after the anodic current density reached a value below 50 nA/cm^2, with a charging current density of -3 mA/cm^2. The oxidation current density versus time was further measured to determine the hydrogen diffusion rate and the corresponding apparent diffusion coefficient (D_{app}), which was determined by fitting the first half of the normalised permeation transient to the analytical solution of Fick's second law [22].

The stress levels of the permeation tests under load are expressed here as a fraction of the yield strength (YS) and will be used to refer to the sample in the following sections. Stresses of approximately 50%, 75%, 100%, and 125% of the YS were applied. The YS was determined by a tensile test performed following the ISO-6892 procedure [23] on an initial gauge length of 80 mm, using the 0.2% strain offset method. This resulted in a value of approximately 700 MPa. Throughout this work, this value will be used as the YS of the considered Q&P steel.

Thermal desorption spectroscopy (TDS) was used to determine the trapping sites present in the material. This technique consists of heating hydrogen-charged samples in an infrared furnace to 850 °C at a constant heating rate of 1200 °C/h. Upon heating, the trapped hydrogen is released from the sample as gaseous H_2 and measured by a quadrupole mass spectrometer (IPI-ESD 100) using a N_2 carrier gas.

Results and discussion

Microstructure characterisation

Depending on processing parameters such as austenitisation temperature, initial quenching temperature and partitioning temperature, different phases and phase fractions can be obtained in Q&P steel. Since the role of austenite as a trapping site for hydrogen is one of the main subjects of investigation in this study, it is important to determine its corresponding phase fraction. The distinction between between fcc austenite and bcc martensite and ferrite was straightforward using the OIM software. Unfortunately, since the c/a ratio of the martensitic phase can be considered close to unity [24], ferrite and martensite are both identified by the software as the same bcc phase. However, using image quality (IQ) a distinction between ferrite and martensite is possible because the high dislocation density in martensite causes a decrease in IQ compared to ferrite. Figure 1 shows a combined phase and IQ map, where the phases are distinguished by colour and the IQ by the grayscale value. Both bcc phases are shown in red, with ferrite appearing lighter due to a higher IQ and martensite darker due to its considerably lower IQ. The austenite volume fraction from EBSD, based on the pixels with a confidence index greater than 0.1, is 7.7 vol%.

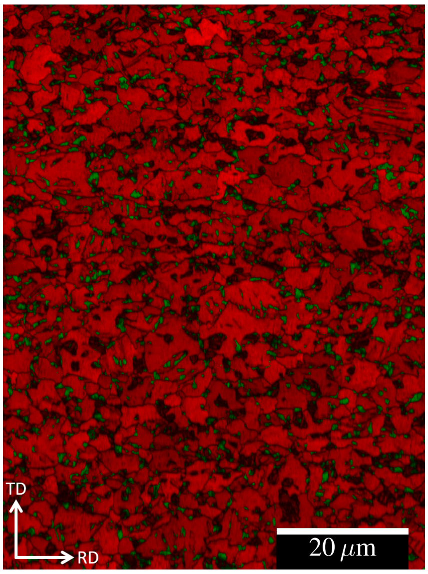

Figure 1: Combined phase-IQ map of the microstructure of the studied Q&P steel (ND-plane). Ferrite (high IQ, bright) and martensite (low IQ, dark) are shown in red, austenite is shown in green.

Similar to EBSD, XRD also distinguishes between fcc and bcc phases using the characteristic diffraction peak positions for certain families of planes for each crystal structure. Using the integrated peak intensity as a measure, an austenite fraction of 11.0 vol% was determined with XRD. The discrepancy in volume fraction of retained austenite determined by EBSD and XRD was expected and could be explained by the different morphologies of retained austenite in Q&P steel [24] and the difference in resolution between both techniques. Retained austenite in Q&P steel is loosely divided into two categories based on size and location. It exists both as filmy austenite, which is situated in between martensite laths and has a size less than approximately 100 nm, and as blocky austenite, which is larger and is situated in the bulk or at the grain boundaries of ferrite and martensite [25]. Therefore, some of the filmy austenite may be too fine to resolve with EBSD and is consequentially not indexed as austenite by EBSD [24].

Effect of load on diffusivity

Several permeation transients (Figure 2a) and their corresponding apparent diffusion coefficients (Figure 2b) were determined using the electrochemical permeation technique. Due to the application of a tensile load, some of the austenite in the material may transform into martensite. This allows to compare the unstressed state to a stressed state, which is more relevant for practical applications, since in service, the steel will often experience external load.

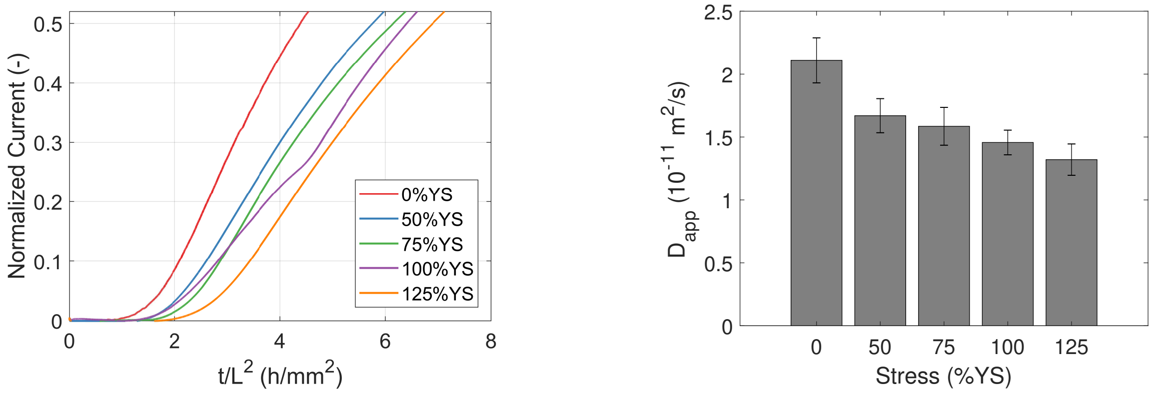

(a) (b)

Figure 2: Electrochemical permeation results for each mechanical loading condition: (a) First half of the normalized permeation transient and (b) the corresponding apparent diffusivity (D_{app}) determined by fitting the first half of each transient to Fick's second law

From the first half of the permeation transients shown in Figure 2a, it can be seen that the samples tested at a constant load all showed a shift to higher times, corresponding to slower diffusion and thus a lower diffusion coefficient, as shown in Figure 2b. Although noticeable, the further decrease in diffusion coefficients with higher applied loads was lower than the decrease observed between the unstressed specimen and the specimen tested at the lowest load (50% YS).

From literature [17, 18], it was expected that purely elastic tensile stresses would increase diffusivity by expanding the lattice without generating dislocations and plastic stresses would decrease diffusivity due to dislocation formation. In this case, however, both elastic and plastic stresses caused a delay in breakthrough time. Since the strain during deformation, especially in early stages, is accommodated mostly by the more ductile ferrite and austenite grains [26–28], the reason behind this observation should be related to increased trapping in the freshly formed martensite upon loading, ferrite or the remaining fraction of retained austenite.

Trapping of hydrogen at retained austenite

In order to determine the trapping sites occupied by hydrogen during the permeation tests under constant load, the specimens used for permeation were tested using TDS. The high temperature end of the resulting spectrum for each testing condition is shown in Figure 3. The specimens are indicated with their corresponding stress level at which the permeation test was carried out. The specimen tested in the same set-up but without load is shown as a reference together with the spectra of the permeation specimens tested under load. It is clear that the spectra of the permeation specimens tested under load additionally contain a high-temperature peak. For the specimen without load, no desorption peak was observed at temperatures higher than 300 °C. Since peaks related to trapping in austenite are usually associated with these higher temperatures [29–31], their absence would imply that without load, the retained austenite is not able to trap hydrogen. It is proposed that further research into this behaviour is done for other combinations of a BCC matrix with retained austenite, e.g. for conventional TRIP-steel. A difference in trapping behaviour could then be related to lower internal stresses in the TRIP-steel due to the softer matrix.

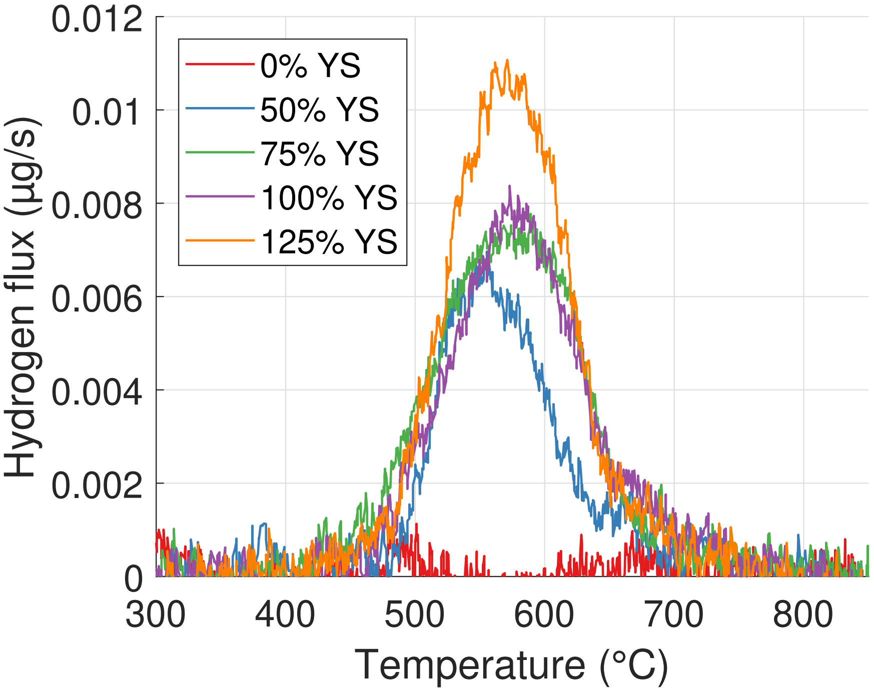

Figure 3: TDS spectra between 300 °C and 800 °C for the specimens tested after electrochemical permeation experiments under a constant load ranging from 0% YS to 125% YS at a heating rate of 1200 °C/h

The result on Q&P-steel can also be linked to the embrittlement observed by Lovicu et al. [6] who also observed no trapping in austenite during conventional charging. During the slow strain rate tensile test, as the load on the retained austenite gradually increases, hydrogen can redistribute itself into the retained austenite. When the retained austenite eventually transforms at higher strains, its dissolved hydrogen is inherited by the newly formed martensite. Consequently, this initiates fracture at the fresh martensite since it is locally supersaturated with hydrogen [12].

Conclusion

This work studied the influence of a constant applied load on the hydrogen diffusion in a Q&P steel containing retained austenite. Trapping was characterised using electrochemical hydrogen permeation and subsequent thermal desorption spectroscopy in order to verify the presence of hydrogen in retained austenite.

- Without external load, the TDS spectra of Q&P steel does not contain a high temperature peak. Therefore, hydrogen is not trapped in the retained austenite under these charging conditions.

- Using electrochemical permeation, it was shown that the diffusivity of hydrogen in quenching and partitioning steels under constant load is slowed down regardless of the level of applied stress (elastic or plastic).

- TDS characterisation of the permeation specimens of Q&P-steel immediately after permeation revealed high temperature trapping sites, which were associated with trapping at retained austenite.

Acknowledgements

The authors gratefully acknowledge the financial support under the scope of the COMET program within the K2 Center "Integrated Computational Material, Process and Product Engineering (IC-MPPE)" (Project No 859480) and from the senior postdoctoral fellowship of TD via the Research Foundation - Flanders (FWO - grant 12ZO420N) and the Special Research Fund (BOF) of UGent (grants BOF15/BAS/062 and BOF20/BAS/121). The COMET program is supported by the Austrian Federal Ministries for Climate Action, Environment, Energy, Mobility, Innovation and Technology (BMK) and for Digital and Economic Affairs (BMDW), represented by the Austrian research funding association (FFG), and the federal states of Styria, Upper Austria and Tyrol.

References

[1] D.V. Edmonds, K. He, F.C. Rizzo, B.C. De Cooman, D.K. Matlock, and J.G. Speer. Quenching and partitioning martensite—a novel steel heat treatment. *Materials Science and Engineering: A*, 438-440:25–34, 2006. Proceedings of the International Conference on Martensitic Transformations.

[2] J. Speer, D.K. Matlock, B.C. De Cooman, and J.G. Schroth. Carbon partitioning into austenite after martensite transformation. *Acta Materialia*, 51(9):2611–2622, 2003.

[3] A. Laureys, T. Depover, R. Petrov, and K. Verbeken. Microstructural characterization of hydrogen induced cracking in trip-assisted steel by ebsd. *Materials Characterization*, 112: 169–179, 2016.

[4] Maoqiu Wang, Eiji Akiyama, and Kaneaki Tsuzaki. Effect of hydrogen on the fracture behavior of high strength steel during slow strain rate test. *Corrosion Science*, 49(11): 4081–4097, 2007.

[5] Motomichi Koyama, Cemal Cem Tasan, Eiji Akiyama, Kaneaki Tsuzaki, and Dierk Raabe. Hydrogen-assisted decohesion and localized plasticity in dual-phase steel. *Acta Materialia*, 70:174–187, 2014.

[6] G. Lovicu, E. Paravicini Bagliani, M. De Sanctis, A. Dimatteo, R. Ishak, and R. Valentini. Hydrogen embrittlement of a medium carbon q&p steel. *Metallurgia Italiana*, 105(6): 3–10, 2013.

[7] Xu Zhu, Wei Li, Hongshan Zhao, Li Wang, and Xuejun Jin. Hydrogen trapping sites and hydrogen-induced cracking in high strength quenching & partitioning (q&p) treated steel. *International Journal of Hydrogen Energy*, 39(24):13031–13040, 2014.

[8] Jilan Yang, Feng Huang, Zhenghong Guo, Yonghua Rong, and Nailu Chen. Effect of retained austenite on the hydrogen embrittlement of a medium carbon quenching and partitioning steel with refined microstructure. *Materials Science and Engineering: A*, 665:76–85, 2016.

[9] George R. Caskey and R.D. Sisson. Hydrogen solubility in austenitic stainless steels. *Scripta Metallurgica*, 15(11):1187–1190, 1981.

[10] X.K. Sun, J. Xu, and Y.Y. Li. *Mater Sci Eng*, 114:179–187, 1989.

[11] Sammy Lap Ip Chan. Hydrogen trapping ability of steels with different microstructures. *Journal of the Chinese Institute of Engineers*, 22(1):43–53, 1999.

[12] JA Ronevich, BC De Cooman, JG Speer, E De Moor, and DK Matlock. Hydrogen effects in prestrained transformation induced plasticity steel. *Metallurgical and Materials Transactions A*, 43(7):2293–2301, 2012.

[13] MI Luppo and J Ovejero-Garcia. The influence of microstructure on the trapping and diffusion of hydrogen in a low carbon steel. *Corrosion science*, 32(10):1125–1136, 1991.

[14] Pengwei Zhou, Wei Li, Hongshan Zhao, and Xuejun Jin. Role of microstructure on electrochemical hydrogen permeation properties in advanced high strength steels. *International Journal of Hydrogen Energy*, 43(24):10905–10914, 2018.

[15] Y.D. Park, I.S. Maroef, A. Landau, and D.L. Olson. Retained austenite as a hydrogen trap in steel welds. *Welding Journal (Miami, Fla)*, 81(2):27/S–35/S, 2002.

[16] D. Pérez Escobar, T. Depover, L. Duprez, K. Verbeken, and M. Verhaege. Combined thermal desorption spectroscopy, differential scanning calorimetry, scanning electron microscopy and X-ray diffraction study of hydrogen trapping in cold deformed TRIP steel. *Acta Materialia*, 60(6):2593 – 2605, 2012.

[17] E. Van den Eeckhout, I. De Baere, T. Depover, and K. Verbeken. The effect of a constant tensile load on the hydrogen diffusivity in dual phase steel by electrochemical permeation experiments. *Materials Science and Engineering: A*, 773:138872, 2020.

[18] W. Zhao, T. Zhang, Z. He, J. Sun, and Y. Wang. Determination of the Critical Plastic Strain-Induced Stress of X80 Steel through an Electrochemical Hydrogen Permeation Method. *Electrochimica Acta*, 214:336–344, 2016.

[19] S. J. Kim and K.Y. Kim. Electrochemical hydrogen permeation measurement through high-strength steel under uniaxial tensile stress in plastic range. *Scripta Materialia*, 66 (12):1069 – 1072, 2012.

[20] M. A. V. Devanathan, Z. Stachurski, and Frederick Clifford Tompkins. The adsorption and diffusion of electrolytic hydrogen in palladium. *Proceedings of the Royal Society of London. Series A. Mathematical and Physical Sciences*, 270(1340):90–102, 1962.

[21] Emilie Van den Eeckhout. *Methodological study of the hydrogen diffusion in steel by means of electrochemical permeation*. PhD thesis, Ghent University, 2019.

[22] Mary D. Archer and N. C. Grant. Achievable boundary conditions in potentiostatic and galvanostatic hydrogen permeation through palladium and nickel foils. *Proc. R. Soc. Lond. A*, 395:165–183, 1984.

[23] ISO 6892-1:2009(E). Metallic materials — Tensile testing — Part 1: Method of test at room temperature. Standard, International Organization for Standardization, Geneva, CH, August 2009.

[24] Grant Thomas, John Speer, David Matlock, and Joseph Michael. Application of electron backscatter diffraction techniques to quenched and partitioned steels. *Microscopy and Microanalysis*, 17(3):368–373, 2011.

[25] X.C. Xiong, B. Chen, M.X. Huang, J.F. Wang, and L. Wang. The effect of morphology on the stability of retained austenite in a quenched and partitioned steel. *Scripta Materialia*, 68(5):321–324, 2013.

[26] Juhua Liang, Zhengzhi Zhao, Di Tang, Nan Ye, Shufeng Yang, and Weining Liu. Improved microstructural homogeneity and mechanical property of medium manganese steel with mn segregation banding by alternating lath matrix. *Materials Science and Engineering: A*, 711:175–181, 2018.

[27] M. Wang and M.X. Huang. Abnormal trip effect on the work hardening behavior of a quenching and partitioning steel at high strain rate. *Acta Materialia*, 188:551–559, 2020.

[28] A. Ebrahimian and S.S. Ghasemi Banadkouki. Mutual mechanical effects of ferrite and martensite in a low alloy ferrite-martensite dual phase steel. *Journal of Alloys and Compounds*, 708:43–54, 2017.

[29] L. Claeys, V. Cnockaert, T. Depover, I. De Graeve, and K. Verbeken. Critical assessment of the evaluation of thermal desorption spectroscopy data for duplex stainless steels: A combined experimental and numerical approach. *Acta Materialia*, 186:190–198, 2020.

[30] Y. Yagodzinskyy, O. Todoshchenko, S. Papula, and H. Hänninen. Hydrogen solubility and diffusion in austenitic stainless steels studied with thermal desorption spectroscopy. *steel research international*, 82(1):20–25, 2011.

[31] M. Enomoto. Simulation of thermal desorption spectrum of hydrogen from austenite embedded in the martensite matrix. *International Journal of Hydrogen Energy*, 42(15): 10579–10590, 2017.